

Microstructure and electrical properties of (Ta, Co, Pr) doped TiO₂ based electroceramics

V. C. Sousa[✉], M. M. Oliveira[✉], M. O. Orlandi[✉],
E. Longo

Received: 25 November 2008 / Accepted: 15 April 2009 / Published online: 3 May 2009
Springer Science+Business Media, LLC 2009

Abstract The addition of different dopants affects the several TiO₂-based varistors are already known [1]. densification, mean grain size and electrical properties of however, their electrical properties still need to be TiO₂-based varistor ceramics. This paper discusses the improved. Several studies have demonstrated that oxides microstructural and electrical properties of (Ta, Co, Pr) with the general MO formula tend to act as densifying doped TiO₂ systems, demonstrating that some of these agents [2] and dopants with a 5 valence, such as Nb and systems display electrical properties that allow for their use as Ta, readily dissolve in the TiO₂ lattice, reducing its resistance as low voltage varistor. Dopants such as Ta play a role by trapping electrons in the band gap. Other oxides special role in the formation of barriers at the grains such as Cr₂O₃ and Bi₂O₃ also improve the electrical boundary and in the nonlinear behavior in TiO₂-based characteristics [3, 5, 8]. systems. The higher values of nonlinear coefficient and This work proposes to investigate how some dopants breakdown electric field were obtained in the system just (Ta, Co, Pr) change the electrical and microstructural properties of TiO₂-based systems and the correlation between microstructure and nonohmic properties.

1 Introduction

TiO₂-based varistor ceramics doped with oxides such as Ba, Bi, Cr, Ta and Nb can display properties appropriate for low voltage varistor applications. The physical and electrical properties and microstructural characteristics of

2 Materials and methods

The powders were obtained by conventional oxide mixing method using the following compounds: TiO₂ (Merck), Ta₂O₅ (Merck), CoO (vetec), and Pr₂O₃ (Aldrich). The molar compositions studied were: (TC) 99.98% TiO₂ + 0.02% CoO (TT) 99.750% TiO₂ + 0.250% Ta₂O₅ (TTC) 99.730% TiO₂ + 0.250% Ta₂O₅ + 0.020% CoO (TTCP 1) 99.705% TiO₂ + 0.250% Ta₂O₅ + 0.020% CoO + 0.025 Pr₂O₃ (TTCP 2) 99.680% TiO₂ + 0.250% Ta₂O₅ + 0.020% CoO + 0.050 Pr₂O₃. The material was blended for 6 h in a ball mill, using isopropyl alcohol as the dispersion medium and butyl polyvinyl alcohol (PVB) as defloculant. After homogenization, each blend was oven-dried at 60 °C for 12 h, and then forced to pass through a 200-mesh sieve (with 74 μm openings). The powders thus obtained were isostatically pressed at 150 MPa into tablets (10 mm diameter by 1 mm thickness). These tablets were sintered in a MAITEC furnace at 1,400 °C for 2 h after which they were cooled to room temperature at cooling rate

V. C. Sousa (✉)
Federal University of Rio Grande do Sul, UFRGS, DEMAT,
Campus do Vale. Av. Bento Gonçalves, 9500, Setor 4, P. 74,
1 andar, S. 213 91, Porto Alegre, RS 509-900, Brazil
e-mail: vania.sousa@ufrgs.br

M. M. Oliveira
CEFET-MA/DAQ, Av. Getúlio Vargas, 04, 65030-005,
São Luís, MA, Brazil

M. O. Orlandi
UNESP/Ilha, Solteira, SP, Brazil

E. Longo
CMDMC, LIEC, DQ, UNESP, Araraquara, SP, Brazil

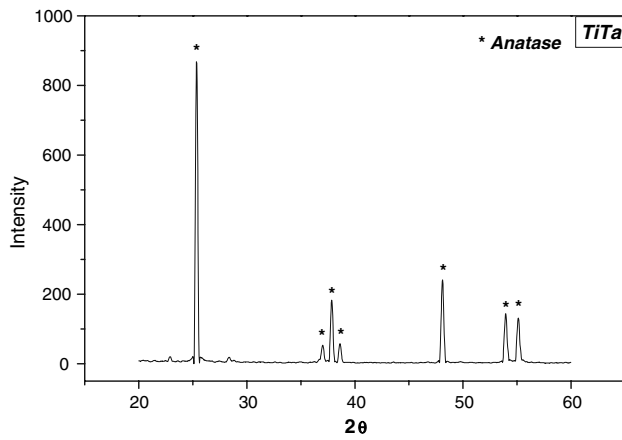


Fig. 1 Diffraction pattern of the powder of the TiO₂-Ta₂O₅ system

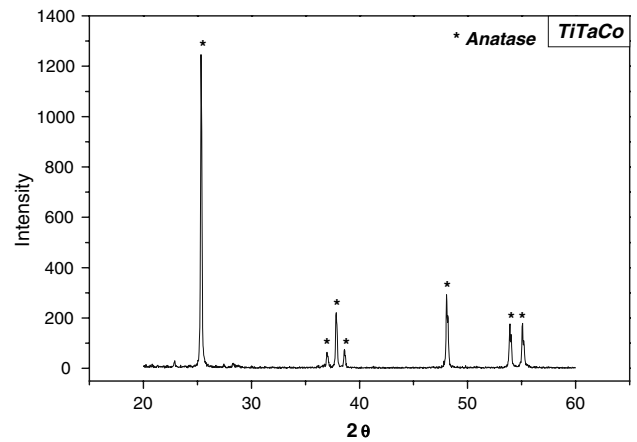


Fig. 3 Diffraction pattern of the powder of the TiO₂-Ta₂O₅-CoO system

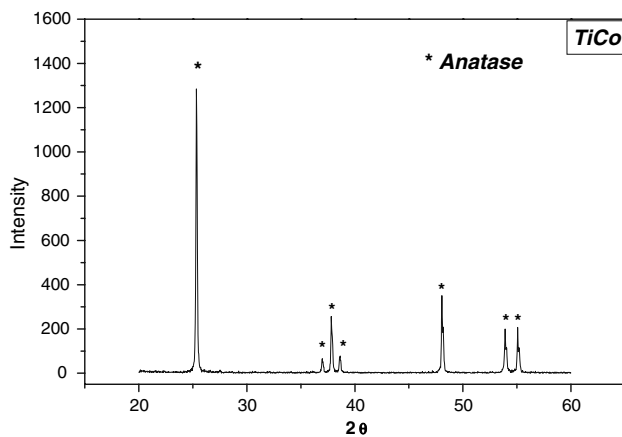


Fig. 2 Diffraction pattern of the powder of the TiO₂-CoO system

Table 1 Effect of the addition of Ta, Co, and Pr oxides on the apparent density (D) and percentage of theoretical density (Dr) of TiO₂

System	Density (g/cm ³)	Dr (%)
TiO ₂ -Ta ₂ O ₅ (TT)	4.13	97.29
TiO ₂ -CoO (TC)	4.16	97.79
TiO ₂ -Ta ₂ O ₅ -CoO (TTC)	4.13	97.20
TiO ₂ -Ta ₂ O ₅ -PrCoO-025P ₂ O ₃ (TTCP1)	4.10	96.88
TiO ₂ -Ta ₂ O ₅ -PrCoO-050P ₂ O ₃ (TTCP2)	4.16	98.38

of 10 C/min. The phases were identified by X-ray diffraction (XRD), using a SIEMENS D-5000 diffractometer. Morphological characterization was made using a scanning electron microscopy (SEM) (Zeiss, model DSM 240 A) with energy dispersive X-Ray spectroscopy stage attached to the microscope. For SEM images the samples were polished with diamond paste and coated with a thin gold film for electrical conductivity.

To electrically characterize them, the tablets were polished to reduce their thickness to 1mm and then metallized by depositing a silver ink coating on their parallel surfaces. They were then heat treated at 400 for 20 min to ensure the oxidation of the electrodes. Their varistor properties were appraised by analyzing their nonlinear coefficient (α) and breakdown electric field (E_b). The α value was calculated from the characteristic curve of current density (j) as a function of the applied electric field (E), and was obtained with a high voltage source (KEITHELEY, model 237), using a linear regression of the ln j-E curve on a logarithmic scale to determine the value of α starting from 1 mA/cm².

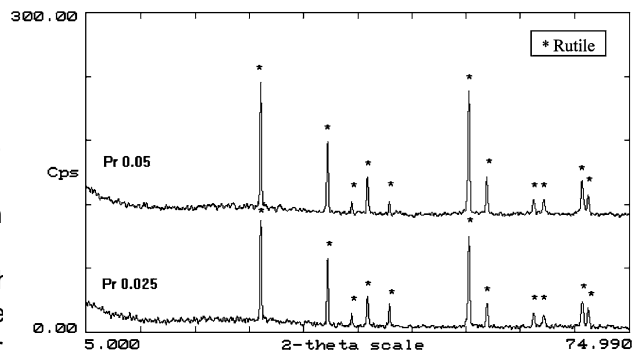


Fig. 4 X-ray diffraction patterns of the TTCP1 and TTCP2 systems after sintering at 1,400°C

Results and discussion

Figures 1, 2 and 3 show the X-ray diffraction patterns of the powders taken after the mixture of the TiO₂-Ta₂O₅ (TT), TiO₂-CoO (TC) and TiO₂-Ta₂O₅-CoO (TTC) systems. Note that no other phase but anatase, the characteristic phase of TiO₂ below 600 C, was detected in this analysis.

Table 1 shows the variation in density of the samples after sintering at 1,400°C for 2 h. Note that the CoO tends to contribute more toward increasing the density of the

TiO₂ than does the Ta₂O₅. According to the literature [9, 10], metal oxides with the general MO formula usually act as TiO₂ densifying agents. This behavior can be explained by the formation of solid solution, according to the reaction (1).



formed, allowing for diffusion through the TiO₂ lattice and the resulting densification.

CoO has also been used as a densifying agent in studies involving SnO₂ varistors [11], where it proved essential for the densification of SnO₂.

As can be seen, for each metallic ion M⁽²⁾ in solid solution, an oxygen vacancy is

Fig. 5 Microstructure and energy dispersive X-ray spectroscopy (EDX) of the TiO₂:Ta₂O₅:CoO system doped with 0.05%(mol) of Pr₂O₅ (TTCP1)

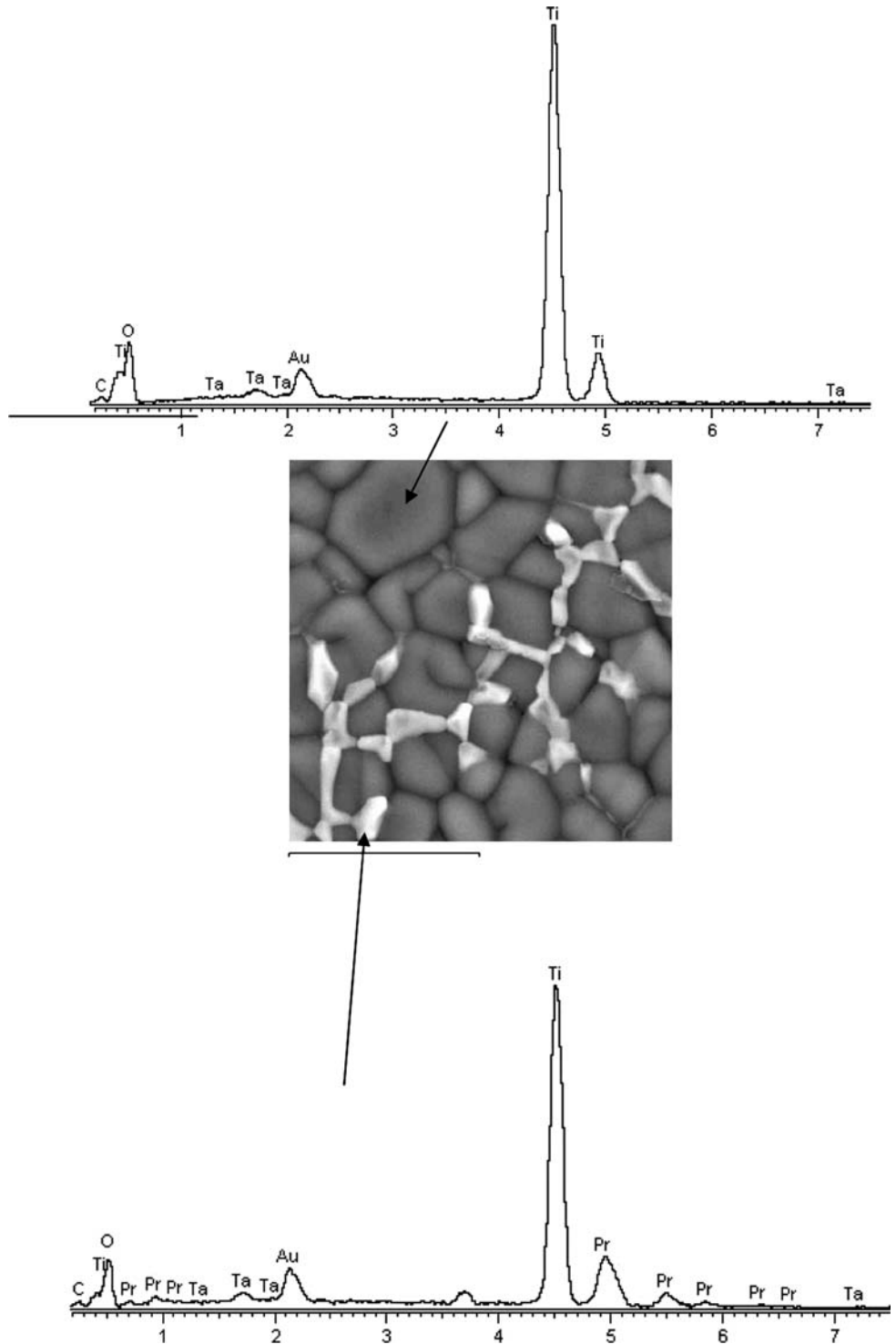


Fig. 6 Microstructure and energy dispersive X-ray mapping of the $\text{TiO}_2\text{-Ta}_2\text{O}_5\text{-CoO}$ system doped with 0.05% (mol) of P_2O_5 (TTCP2)

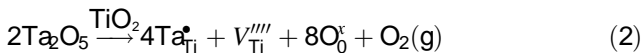
On the other hand, it was found that the simultaneous addition of tantalum and cobalt oxides tended to mask the densifying action of CoO , although the alteration was more to the densification of the TTC system than did the addition of the same proportion of chromium oxide. The table values indicates that the addition of more than 0.025% (mol) of praseodymium oxide tended to contribute

Figure 4 shows the X-ray diffractogram patterns of the (a) TTCP 1 and (b) TTCP2 samples after sintering at 1,400 C. X-ray diffractometry (Fig4) revealed that, after sintering at 1,400C, all the compositions showed only the presence of the rutile phase of TiO₂. This result was expected due to the fact this is the most stable phase of TiO₂ at higher temperatures. Titania normally undergoes anatase-rutile phase transformation in the temperature range 600D700C [12].

Energy dispersive X-ray spectroscopy (EDX) coupled to scanning electron microscopy (SEM) (Figs. 6) allowed us to detect the presence of Pr and oxygen precipitated in the region of the grain boundary of systems TTCP1 and TTCP2. However, the X-ray diffractometry (Fig) revealed that all the compositions showed only the presence of the rutile phase of TiO₂. Therefore, phases with praseodymium oxide were not detected. This result was expected due to the fact that the dopant concentration was below the diffractometer's detection limit.

The TTCP1 system containing the lowest concentration of Pr oxide and analyzed by SEM (Fig7a) showed a dense system, confirming the results of Archimedes. On the other hand, an increase in the praseodymium oxide concentration (Fig. 7b; Table1) tended to reduce the porosity and increase the density. X-ray mapping (Fig. 6) of this composition revealed the presence of adsorbed oxygen and Pr at the grain boundaries, which favors the electrical properties, increasing the nonlinear coefficient and the breakdown electric field, as shown in Table 2.

As can be seen from the tension curve as a function of the current, the TiO₂CoO (TC) system displays a resistive behavior, therefore, was not possible to determine the nonlinear coefficient and breakdown electric field value (Fig. 8). On the other hand, the addition of tantalum oxide (TTC) to the system causes it to show varistor properties: with a nonlinear coefficient of 6 and a breakdown electric field of 79 V/cm (Fig.8 and Table2), presumably related with the increase in conductivity of the grain produced by the replacement of TiO₂ for Ta₂O₅. This result illustrates the importance of tantalum oxide in the formation of nonlinear behavior in TiO₂-based systems. In some studies [7, 13], it has been observed that the replacement of Ta⁵⁺ for Ti⁴⁺ promotes the formation of defects (E₂), creating depletion layers at the grain boundaries and leading to the formation of a potential barrier for electronic transport, which favors semiconductor behavior.



The addition of Pr₂O₃ to the ternary TiO₂Ta₂O₅CoO system in the concentrations studied here (Table 1, Fig. 9) did not favor the varistor properties of the TiO₂-based system, unlike what has been reported for Sr₂CoO₅-based

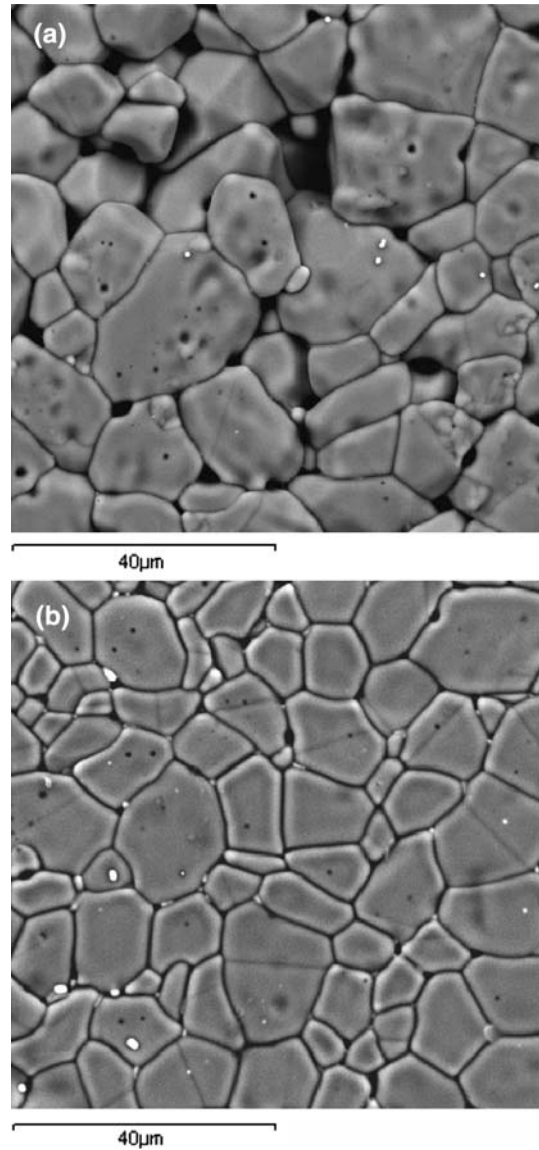


Fig. 7 Microstructure of the TiO₂Ta₂O₅CoO system doped with a 0.025% (mol) and b 0.05% (mol) of Pr₂O₃

Table 2 Grain size, non-linear coefficients (α) and breakdown electric field (E_b), of the TTC, TTCP1 and TTCP2 systems sintered for 2 h and cooled at a rate of 10°C/min

Sample	α	E _B (V/cm)	Grain size (µm)
TTC	6.1	79	2.8
TTCP1	3.7	38	9.9
TTCP2	5.6	62	8.2

systems [14]. The two Pr₂O₃ concentrations showed lower values of α than the system without Pr₂O₃. This α value reducing effect caused by the addition of Pr₂O₃ is likely due to the fact that the Pr₂O₃ is precipitated in the grain boundary region (Figs. 6, 7), and does therefore not contribute toward

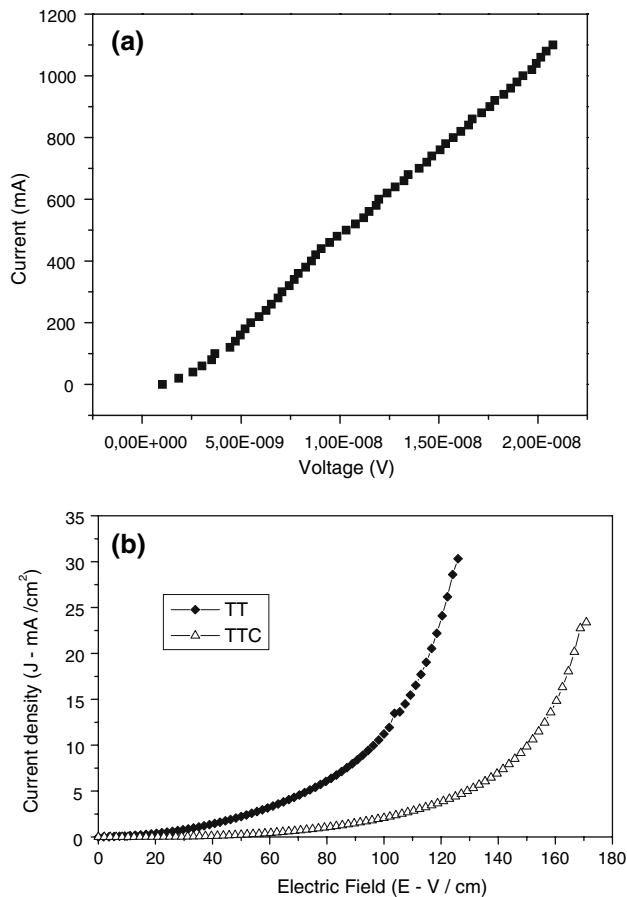


Fig. 8 a Current as a function of the system's voltage TC-without Ta_2O_5 and b density current as a function of the electric field of the TT and TTC systems with Ta_2O_5 and CoO

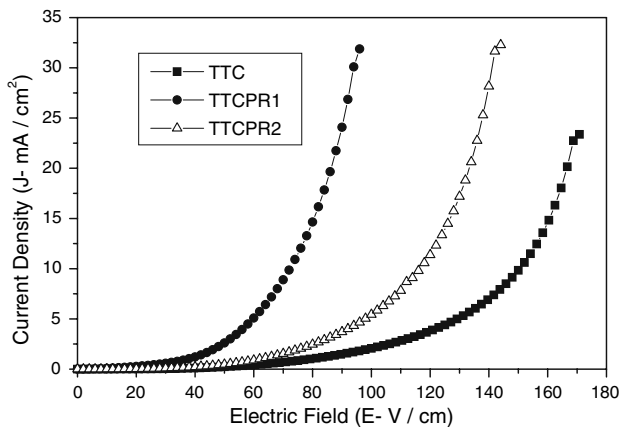


Fig. 9 Effect of the praseodymium oxide on the curves behavior of the current density as a function of the electric field

the formation of an effective potential barrier. This deleterious effect of precipitates in the grain boundary region on the electrical properties of varistors has also been observed in SnO₂-based systems [5]. A reduction in the breakdown electric field value was observed, and is likely related with the increase in mean grain size.

4 Conclusion

At the concentrations used in this study, it was found that CoO and Pr tend to act as densifying agents in TiO₂-based varistors, but do not tend to contribute to the electrical properties of these varistors. Only Pr_2O_3 favored the nonohmic behavior of the systems studied here. The presence of praseodymium oxide precipitated at the grain boundaries is one of the possible explanations for the deleterious effect of this oxide on the electrical properties.

References

1. M.F. Yan, W.W. Rhodes, *Appl. Phys. Lett.* **40**, 536 (1982). doi: 10.1063/1.93134
2. S.L. Yang, J.M. Wu, *J. Am. Ceram. Soc.* **78**, 2203 (1995). doi: 10.1111/j.1151-2916.1995.tb08637.x
3. J. Pennewiss, B. Hoffmann, *Mater. Lett.* **9**, 219 (1990). doi: 10.1016/0167-577X(90)90134-8
4. M.R.D. Bomio, V.C. Sousa, E.R. Leite, J.A. Varela, E. Longo, *Mater. Chem. Phys.* **85**, 96 (2004). doi:10.1016/j.matchemphys.2003.12.015
5. P.R. Bueno, E. Camargo, E. Longo et al., *J. Mater. Sci.* **16**, 2048 (1996)
6. J.J. Cheng, J.M. Wu, *Mater. Chem. Phys.* **48**, 129 (1997). doi: 10.1016/S0254-0584(97)80106-X
7. V.C. Sousa, E.R. Leite, J.A. Varela, E. Longo, *J. Eur. Ceram. Soc.* **22**(8), 1277 (2002)
8. V.C. Sousa, M.R. Cassia-Santos, C.M. Barrado, R.M.D. Bomio, E.R. Leite, J.A. Varela, E. Longo, *J. Mater. Sci.: Mater. Electron.* **15**, 665 (2004). doi:10.1023/B:JMSE.0000038921.07744.9d
9. J.M. Wu, C.H. Lai, *J. Am. Ceram. Soc.* **74**(12), 3112 (1991)
10. P.H. Duvigneaud, D. Reinhard, *Sci. Ceram.* **12**, 287 (1980)
11. S.A. Pianaro, P.R. Bueno, E. Longo, J.A. Varela, *J. Mater. Sci. Lett.* **14**, 692 (1995). doi:10.1007/BF00253373
12. C. Suresh, V. Biju, P. Mukundan, K.G.K. Warrier, *Polyhedron* **17**(18), 3131 (1998)
13. C.P. Li, J.F. Wang, W.B. Su, H.C. Chen, Y.J. Wang, D.X. Zhuang, *Mater. Lett.* **57**, 1400 (2003). doi:10.1016/S0167-577X(02)00996-5
14. M.M. Oliveira, P.R. Bueno, E. Longo, J.A. Varela, *Mater. Chem. Phys.* **1**, 9182 (2001)
15. P.R. Bueno, E.R. Leite, M.M. Oliveira, M.O. Orlandi, E. Longo, *Appl. Phys. Lett.* **79**(1), 48 (2001)